

Study on the Optimization of Surface Modification Processing of SiC_p and Tribological Properties of AA6061-SiC_p based Composites

Odiwo H., Bello K.A., Abdulwahab M., Adebisi A.A., Abdullahi U., Dodo R.M., Maleque M.A. and Suleiman M.U.



Received: 23 November 2022
Accepted: 04 January 2023
Published: 20 January 2023
Publisher: Deer Hill Publications
© 2023 The Author(s)
Creative Commons: CC BY 4.0

ABSTRACT

The unique property combination of Al/SiC_p based composites make them very attractive for applications in automotive and aerospace industries. The choice of composite materials for these applications is directly influenced by their inherent properties which are a function of the processing route employed. Like other processing parameters, surface modification treatment of SiC_p can play a major role in determining the properties of Al/SiC_p composites. In this study, the effects of SiC reinforcement (wt%) fractions (SRF), surface oxidation temperature (SOT) and preheating temperature (PT) parameters on the wear and friction properties of stir-cast Al-SiC_p based composite were investigated. Experimental data and models are generated and analyzed based on a three-factors-five-level central composite design (CCD) and analysis of variance (ANOVA). The empirical models developed for wear rate and coefficient of friction (COF) considering the pre-processing parameters adequately predicts the Al-SiC_p properties with the silicon carbide reinforcement (wt%) fraction emerged as the most influencing factor. The goal of the optimization process is to minimize both wear rate and COF. For wear rate, SRF at 44.49 % contribution had the most influence on wear rate, while SOT and PT had 0.65 % and 1.03 % influence on wear rate respectively. For COF, SRF also showed highest influence of 35.48 % on COF, while SOT and PT had 0.047% and 2.66% influence on COF respectively. From the optimization analysis, the set of conditions that simultaneously optimizes both wear rate and COF are 10% SiC weight (SW), 1234°C surface oxidation temperature (SOT), and 376.2°C preheat temperature (PT). The resulting responses at this optimized condition are minimum wear rate of 0.11 mm³/m and COF of 0.11 with a confidence and desirability level of 1.

Keywords: Aluminium-silicon carbide composite, surface oxidation, preheat temperature, central composite design.

1 INTRODUCTION

Conventional monolithic aluminium alloys fail to meet the rising demand for high performance structural applications due to their low strength and low wear resistance properties (Moses *et al.*, 2016). In the last few decades, the use of ceramic particles in the strengthening of aluminium has been gaining significant popularity (Alten *et al.*, 2019). Ceramic particulates like SiC, B₄C, TiC, WC, ZrO₂ and Al₂O₃ are the commonly used reinforcements to fabricate aluminium matrix composites, (AMCs), (Nagaral *et al.*, 2016). As a result of its excellent thermal conductivity, good corrosion resistance, high modulus and strength, low cost, availability, and suitable compatibility with aluminium alloys, silicon carbide (SiC) is the most commonly used ceramic material for composite reinforcement. They have emerged the most preferred materials for composite production as indicated in Figure 1 because they are well suited for excellent heat and wear resistance applications (Bobic *et al.*, 2010; Adebisi *et al.*, 2016; Odiwo *et al.*, 2021).

Silicon carbide reinforced aluminium matrix composites (AMCs) have been widely used in automobile and aerospace applications for production of engine parts such as piston, connecting rod and brake drum where sliding contact is important due to their low density, high strength, high stiffness, good corrosion resistance and high wear resistance properties in comparison with monolithic aluminium alloys. Excessive wear of the mating components during operation leads to catastrophic failures (Nagaral *et al.*, 2016; Verma & Khvan, 2019).

Odiwo H.✉, Bello K.A.^a, Abdulwahab M.^{a,b}, Adebisi A.A.^{a,b}, Abdullahi U.^c, Dodo R.M.^a, Maleque M.A.^d and Suleiman M.U.^a

^aDepartment of Metallurgical and Materials Engineering, Ahmadu Bello University, Zaria-Nigeria.

^bDepartment of Metallurgical and Materials Engineering, Air Force Institute of Technology, Kaduna-Nigeria.

^cCentre for Energy Research and Training, Ahmadu Bello University, Zaria-Nigeria.

^dDepartment of Manufacturing and Materials Engineering, International Islamic University Malaysia, Kuala Lumpur, Malaysia
E-mail: hammedodiwo@gmail.com

Reference: Odiwo et al. (2023). Study on the Optimization of Surface Modification Processing of SiC_p and Tribological Properties of AA6061-SiC_p based Composites. *International Journal of Engineering Materials and Manufacture*, 8(1), 1-12.

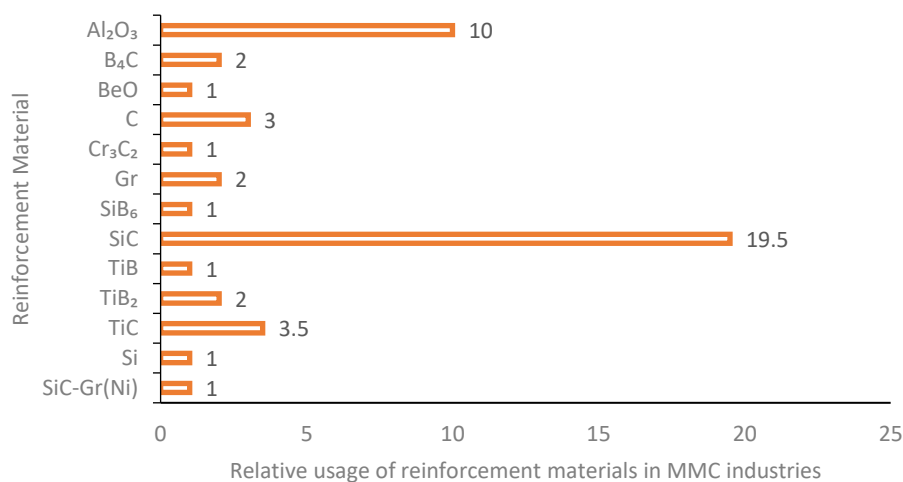


Figure 1: Industrial usage of reinforcement materials (Odiwo *et al.*, 2021)

Many techniques are available for the fabrication of aluminium/silicon carbide particulate composites such as spray deposition, powder metallurgy, infiltration technique, squeeze casting and stir casting. However, stir casting is one of the most commonly used method to fabricate aluminium matrix composites because of its simplicity, ease of production of complex casting, mass production possibility and it is economical (Ramesh *et al.*, 2010). The main factors controlling the properties of MMCs fabricated using stir casting techniques include reinforcement distribution, wetting of reinforcement by the matrix aluminium alloy, reactivity at the reinforcement / matrix interface and porosity in the solidified casting. These factors are directly influenced by the casting processing parameters such as processing temperature, stirring time, stirring speed, preheat temperature, blade angle, melt temperature, particle feed rate, etc. When these parameters are well controlled, the factors are significantly improved and Al-SiC_p composites of better properties are produced (Adebisi *et al.*, 2017; Verma & Khvan, 2019; Adediran *et al.*, 2021).

Adebisi and Ndaliman (2015) studied the influence of process parameters (reinforcement fraction, stirring speed, processing temperature and processing time) on wear and density properties of AA6061-SiC_p composites produced using stir casting. Stirring speed and processing time are reported as the most influential parameters and were able to obtain a wear mass loss as low as 1×10^{-3} g and density value achieved as high as 2.780g/mm³ using the optimum parametric combination of 14 wt.% reinforcement fraction, 460 rpm stirring speed, 820 °C processing temperature and 150 seconds processing time. Umanath *et al.*, (2013) studied the wear behavior of Al6061/SiC/Al₂O₃ hybrid metal matrix composites with volume fraction, applied load, rotational speed and counter-face hardness as the process parameters. Among the four parameters, volume fraction and counter-face hardness had the most influence on reduction of wear rate of the hybrid composites. Rana *et al.*, (2017) developed a mathematical model to study the influence of process parameters (casting temperature, stirrer speed, and weight percent of reinforcement) on hardness of AA5083/Nano-SiC composite fabricated by stir casting. Optimum hardness of 19.4 HBN was obtained using the optimized process parameters 2wt.% of nano-SiC, 760 °C casting temperature and 550 rpm stirrer speed generated from the model.

The common practice of evaluating material integrity is done by studying one factor at a time. Such practice is unable to evaluate the material effectively since the study did not include the interactions amongst the factors. Whether the interaction effect is significant or not, each of the factors contribute to material integrity. Along these lines, it is important to utilize the design of experiments (DOE) in the investigation because of its capacity in estimating the connections between the factors (Ahmad *et al.*, 2020). Central composite design (CCD) of response surface methodology (RSM) is a very efficient method in reducing the number of experiments with a large number of factors and levels. It provides high quality predictions in studying linear, quadratic and interaction effects of factors influencing a response. CCD is also capable of achieving the optimum conditions required to attain the best characteristic properties (Montgomery, 2013; Myers *et al.*, 2016).

Therefore, the aim of this study is to investigate the influence of particle pre-processing parameters surface oxidation and preheat temperature of varying SiC_p addition on the tribological properties of Al-SiC_p composites.

2 EXPERIMENTAL DETAILS

2.1 Materials and Method

AA6061 aluminium alloy used as the matrix was produced using stir casting method and the composition of the as-cast alloy is given in Table 1. Silicon carbide (SiC_p) powder of 76 μm was employed to reinforce the aluminium alloy. The properties of the matrix aluminium (AA6061) alloy and the silicon carbide (SiC_p) powder are highlighted in Table 2.

Table 1: Composition of as-cast AA6061 alloy

Si	Cu	Mn	Mg	Cr	Zn	Ti	Al
0.62	0.22	0.03	0.84	0.22	0.10	0.10	Balance

Table 2: Properties of AA6061 alloy and SiC_p (Adebisi *et al.*, 2017)

Property	Unit	AA6061	SiC _p
Density	g/cm ³	2.7	3.22
Melting point	°C	660	2973
Coefficient of thermal expansion	μm/m°C	23.4	4
Thermal conductivity	W/mK	166	126
Young's modulus	GPa	70	410

SiC particles (SiC_p) were exposed to surface oxidation and preheating pretreatment operations prior to composite production. For the surface oxidation pretreatment, the SiC_p are heated to temperatures above 1000 °C so that thin layer of silica (SiO₂) is formed on its surface. SiO₂ layer acts as a barrier preventing the direct contact between SiC_p and aluminium alloy during composite production (Khalid *et al.*, 2013). The SiC_p samples to be oxidized were weighed in alumina crucible using the 0.0001g precision weighing balance and then placed in an electric resistance furnace already set to the temperature required for surface oxidation. Five samples of the measured SiC_p were pretreated at high temperature of 1100 °C, 1150 °C, 1200 °C, 1250 °C and 1300 °C respectively. The furnace was set to heat the samples at a heating rate of 10 °C/min. After attainment of the desired temperatures, SiC_p samples were held at each temperature for 2hrs and then allowed to cool in air (Vantrinh *et al.*, 2018 and Lee *et al.*, 2020).

Preheating of oxidized-SiC_p at temperatures relatively much lower than the oxidation temperatures is a process performed to assist in obtaining increased wettability between the molten aluminium alloy and the oxidized-SiC_p during composite production. After weighing the oxidized-SiC_p samples, the graphite crucible was placed in the electric resistance furnace and heated to temperature of 300 °C, 350 °C, 400 °C, 450 °C and 500 °C based on the experimental requirement in the central composite design matrix. After reaching the required temperature, sample were allowed to homogenize for 30 minutes in the furnace and then added into the molten alloy.

Melting of the AA6061 alloy was achieved using the copular furnace. The dross (solid mass of impurities floating on molten metal) formed was skimmed off to obtain higher purity of the AA6061 alloy. Afterwards, the oxidized-SiC_p were preheated at the required temperature (300 °C, 350 °C, 400 °C, 450 °C or 500 °C) for 30 minutes and then carefully added into the vortex of the molten alloy created mechanical stirring. The mixture was maintained at a temperature of about 710 °C and further stirred for 2 minutes at a stirring speed of 500 rpm using a stainless steel stirrer before being poured into the Ø20 mm by 110 mm prepared cylindrical sand mold. The weight fraction of the SiC_p was distributed over 5 levels with 0 and 10 % as the minimum and maximum (i.e. 0, 2.5, 5, 7.5 and 10 %). This process is conducted for each of the experimental runs considering the process parameters as suggested by the design plan. After casting, the AA6061/oxidized-SiC_p composite test specimen were prepared for wear measurement.

2.2 Wear and Friction Test

The wear and friction property of the test samples was tested using a ball-on-disk tribometer according to ASTM G99-95 standard. After machining the as-cast composite samples to Ø15 mm x 5 mm dimension, the samples were subjected to metallographic grinding up to P600 grit, cleaned with acetone, dried and weighed using analytical balance with the precision of 0.0001 g. During the wear test, a stainless steel ball of 6 mm diameter was used to as a static partner over a 5 mm radius on the surface of the rotating samples. The load, sliding speed and sliding distance of 8 N, 10 cm/s and 30 m respectively were applied at room temperature, relative humidity of 55 % and a test duration of 30 minutes for all the samples. The value coefficient of friction was automatically generated by the ball-on-disk tribometer during the wear test. After the wear test, the samples were cleaned using acetone, dried and weighed. The wear rats was calculated from the weight loss data obtained using the equation below:

$$w_r = \frac{\text{mass loss}}{\text{sliding distance}} \quad (1)$$

2.3 Experimental Design

The experiments were planned based on CCD method in Design Expert 10 software. It utilized 3-factor-5-level design scheme as shown in Table 3. The factors are SiC reinforcement fraction (SRF), surface oxidation temperature (SOT), and preheat temperature (PT).

Table 3: Factors and levels for the CCD experimental design plan

FACTOR	SYMBOL	LEVEL				
		-2	-1	0	1	2
SiC reinforcement fraction (SRF)	wt.%	0	2.5	5	7.5	10
Surface oxidation temperature (SOT)	°C	1100	1150	1200	1250	1300
Preheat temperature (PT)	°C	300	350	400	450	500

The CCD experimental design plan consist of $2^k + 2k + 6$ runs, where $k = 3$; that is, the number of input factors. The design has 8 factorial points (2^k), 6-star points ($2k$) and 6 central runs to make up a total of 20 experimental runs, i.e. $2^3 + 2(3) + 6 = 8+6+6 = 20$ runs. The experimental run involving only the as-cast AA6061 alloy is excluded from the design since the alloy did not require pretreated SiC reinforcement particles. The experimental outcome is presented in Table 4.

Table 4: Design matrix and responses for oxidized-SiCp reinforced AA6061 matrix composite

Experimental Run	Factors			Responses	
	A: SiC Reinforcement Fraction (wt.%)	B: Surface Oxidation Temperature (°C)	C: Preheat Temperature (°C)	Wear Rate (mm ³ /m)	COF (μ)
1	7.5	1150	350	0.0198	0.670
2	2.5	1150	350	0.042	0.787
3	5	1200	400	0.0272	0.713
4	5	1200	300	0.0321	0.754
5	5	1200	400	0.0284	0.715
6	5	1100	400	0.0321	0.748
7	2.5	1250	350	0.0407	0.766
8	2.5	1250	450	0.037	0.763
9	5	1200	400	0.0272	0.698
10	5	1300	400	0.0309	0.731
11	5	1200	400	0.0272	0.690
12	5	1200	400	0.0333	0.762
13	10	1200	400	0.0111	0.339
14	7.5	1250	350	0.0173	0.495
15	5	1200	400	0.0296	0.717
16	5	1200	500	0.0247	0.679
17	2.5	1150	450	0.0432	0.768
18	7.5	1150	450	0.0185	0.629
19	7.5	1250	450	0.016	0.345

3 RESULTS AND DISCUSSION

3.1 Characterization of As-cast AA6061 Alloy

The SEM micrograph of the as-cast AA6061 alloy in Figure 2 (a) reveals the structure of the eutectic phase containing Mg₂Si in α-aluminium matrix. The Mg and Si in the AA6061 alloy are present as a solid solution phase in the grains and along the grain-boundaries. The prominent peaks corresponding to aluminium, magnesium and silicon in the AA6061 alloy is confirmed by the energy dispersive spectroscopy (EDS) spectra shown in Figure 2 (b). Aluminium is observed to have the highest count than other elements present.

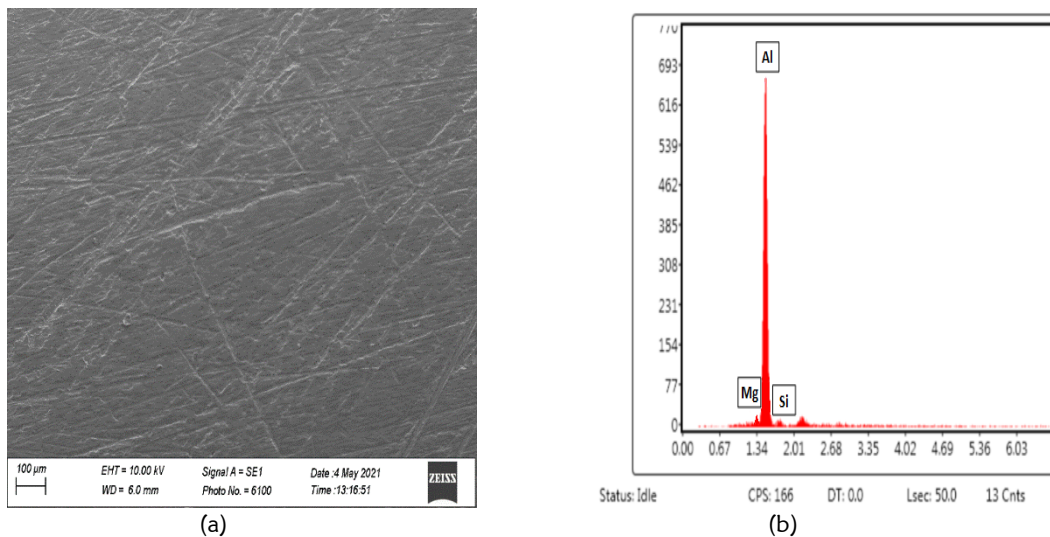


Figure 2: (a) SEM micrograph and (b) EDS of as-cast AA6061 alloy

3.2 Characterization of As-received and Oxidized-SiC_p

SEM-EDS was utilized for the characterization of the as-received SiC_p. The SEM micrograph of the as-received SiC_p in Figure 3 (a) shows the surface of the powder to be very rough with its edges appearing very sharp. EDS spectra in Figure 3 (b) majorly confirmed the presence of silicon and carbon in the particles. When the as-received SiC_p is compared to the 1100 °C-oxidized-SiC_p sample in Figure 4, the surface roughness of the 1100 °C-oxidized-SiC_p is observed to be significantly lower than that of the former. This reduction in surface roughness can be attributed to the thin SiO₂ layer formed on the surface of the SiC_p during surface oxidation treatment which resulted in surface refinement.

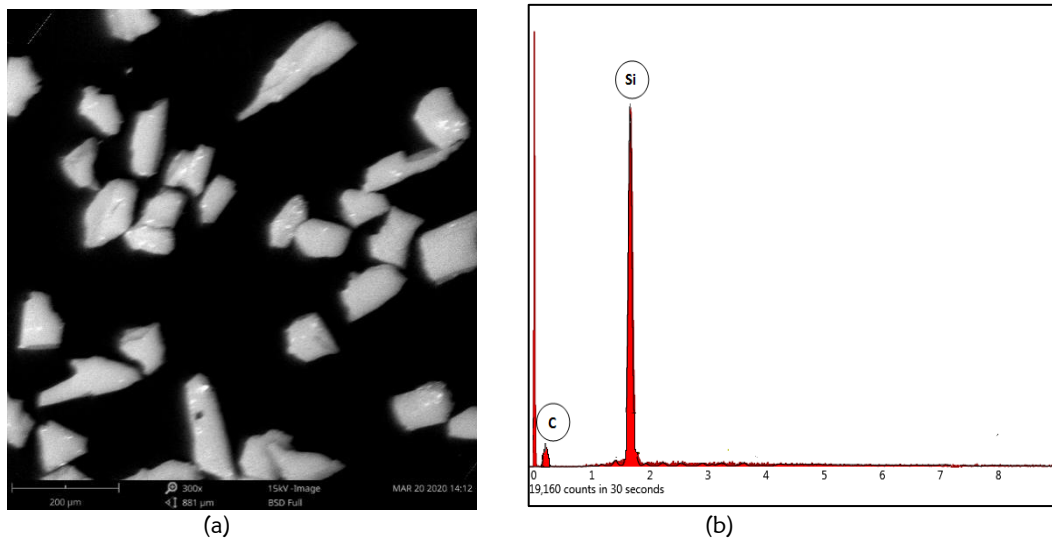


Figure 3: (a) SEM micrograph and (b) EDS of as-received 76 μm SiC_p

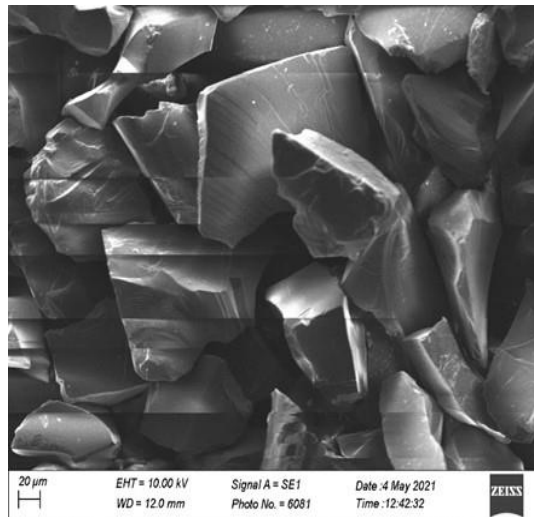


Figure 4: Surface morphology of 1100 °C pre-oxidized SiC_p

The as-received and 1100 °C-oxidized-SiC_p samples were further characterized using X-ray Diffraction (XRD) phase analysis. The XRD spectrum in Figure 5 confirmed the presence of SiC phases in the as-received SiC powder analyzed. The spectrum shows the extensive distribution of SiC phases between 30° and 80° with high peaks observed at 35.72°, 53.93°, 57.54° and 60.22° on the 2θ axis.

From the XRD analysis of the 1100 °C-oxidized-SiC_p sample in Figure 6, the presence of silicon dioxide (SiO₂) coating layer on the SiC_p was further confirmed by the SiO₂ phases observed at diffraction peaks of 22.20°, 31.04°, 31.83° and 32.50° along the 2θ axis.

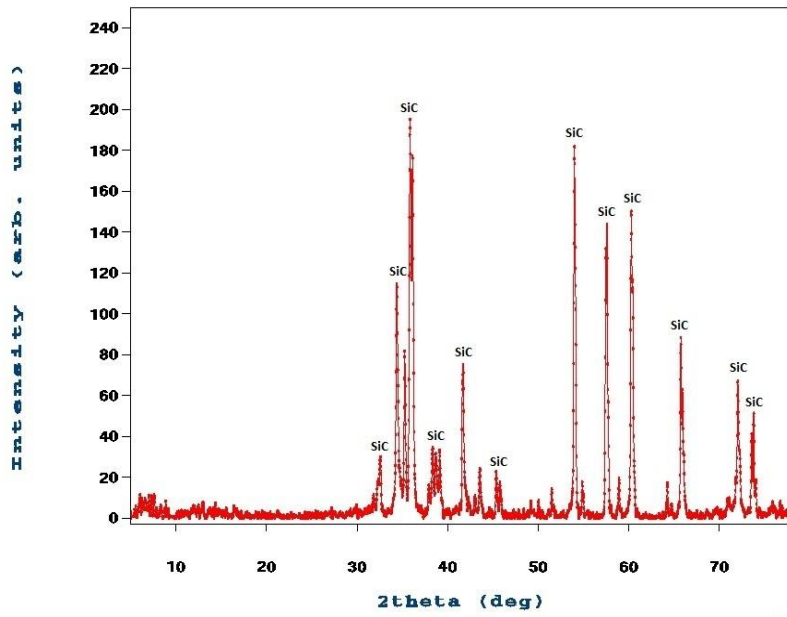


Figure 5: XRD spectrum of as-received SiC_p

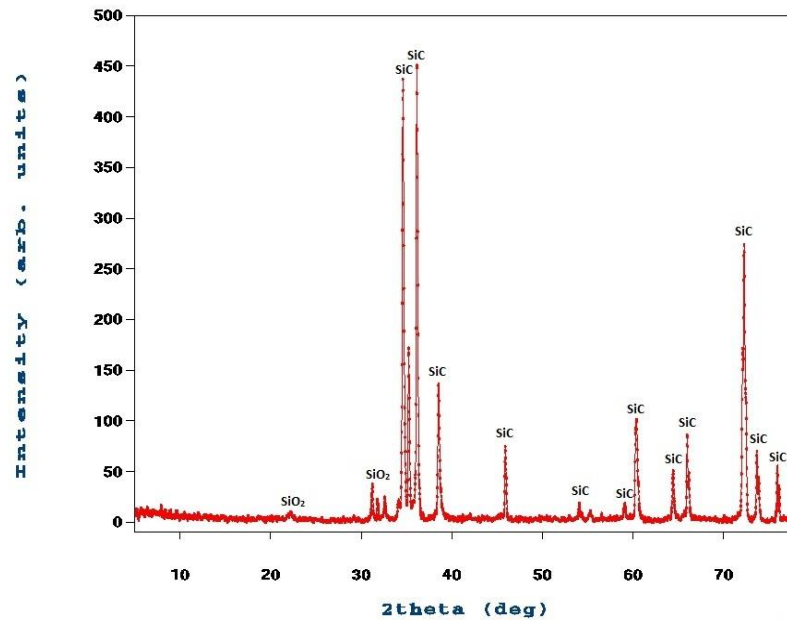


Figure 6: XRD spectrum of 1100 °C-oxidized-SiC_p

3.3 Mathematical Model Development

For model development, the mathematical relationship between the response and the input factors is expressed by the second order polynomial in eqn 2:

From the equation, Y represents the response, X_i and X_j are the equation value of the factors, β₀ is the constant, β_i, β_j and β_{ij} are linear, interaction and quadratic end coefficient respectively, and k is the number of the factors. The experimental results generated after conducting the runs were analyzed using analysis of variance (ANOVA) to confirm the adequacy and validity of the developed model considering the significant model terms. The adequacy and validity is ascertain by confirming the significant terms with p values < 0.05 while model terms with p values > 0.05 are considered insignificant (Di Lio *et al.*, 2020; Adediran *et al.*, 2021).

$$Y = \beta_0 + \sum_{i=1}^k \beta_i X_i + \sum_{i=1}^k \beta_{ii} X_i^2 + \sum_{i=1}^k \sum_{j \geq 1}^k \beta_{ij} X_i X_j + \epsilon \quad (2)$$

3.4 Model for Wear Rate

Fit summary statistics of the model for wear rate is shown in Table 5. The fit summary presents the models to fit experimental data into appropriate model equations which can be first order or linear, second order or quadratic and cubic. From the table, the suggested polynomial for wear rate with F-value of 23.29 at p-value ≤ 0.0001 is significant and quadratic.

Table 5: Fit summary statistics for wear rate

Source	Sum of Squares	df	Mean Square	F Value	p-value (Prob > F)	
Mean	30238.63	1	30238.63			
Linear	4443.25	3	1481.08	39.91	< 0.0001	
2FI	22.89	3	7.63	0.17	0.9136	
<u>Quadratic</u>	<u>472.83</u>	<u>3</u>	<u>157.61</u>	<u>23.29</u>	<u>0.0001</u>	<u>Suggested</u>
Cubic	25.42	4	6.35	0.90	0.5295	Aliased
Residual	35.49	5	7.10			
Total	35238.51	19	1854.66			

Analysis of variance (ANOVA) for wear rate carried out at 5 % significance level is presented in Table 6. It is observed from the table that the model is significant with a p-value of 0.0001 which is less than 0.05 and F-value of 141.07. Values of Prob > F less than 0.0500 indicate model terms are significant. In this case, A, B, C and A² are statistically significant model terms since their p-values are less than 0.05, while, AB and B² are insignificant terms retained in the ANOVA because they help in reducing the model terms of the input factors (A, B & C) to their present p-value. Other model terms AC, BC and C² were removed for model reduction. Furthermore, the p-value of the lack of fit which corresponds to 0.6647 is greater than 0.05 indicating that the lack of fit is non-significant which is desirable for model adequacy.

Table 6: Analysis of variance for wear rate

Source	Sum of Squares	Df	Mean Square	F Value	p-value (Prob > F)	
Model	4929.99	6	821.66	141.07	< 0.0001	significant
A-SiC reinforcement fraction	2224.60	1	2224.60	381.94	< 0.0001	
B-Surface oxidation temp	32.50	1	32.50	5.58	0.0359	
C-Preheat temp	51.51	1	51.51	8.84	0.0116	
AB	15.42	1	15.42	2.65	0.1297	
A ²	440.56	1	440.56	75.64	< 0.0001	
B ²	17.77	1	17.77	3.05	0.1062	
Residual	69.89	12	5.82			
Lack of Fit	34.40	7	4.91	0.69	0.6829	not significant
Pure Error	35.49	5	7.10			
Cor Total	4999.88	18				

Also, the difference between the predicted R² (0.9532) and adjusted R² (0.9790) of the model is less than 0.2, which establishes the reasonable agreement required for model adequacy. The model equation developed for the prediction of wear rate for any given level of each of the process parameters in the experiment is presented in equations 3.

$$\frac{1}{\text{wear rate}} = -429.02212 - 16.52776 \times \text{SRF} + 0.76392 \times \text{SOT} + 0.03588 \times \text{PT} + 0.01110 \times \text{SRF} \times \text{SOT} + 0.94905 \times \text{SRF}^2 - 3.29557E - 004 \times \text{SOT}^2 \quad (3)$$

Equation 4 is used to identify the relative impact of the processing parameters by comparing their coefficients. From the equation, it is concluded that the process parameter with the most influence on wear rate is SiC reinforcement fraction (SRF). SRF had 44.49 % influence on wear rate, while SOT and PT had 0.65 % and 1.03 % influence on wear rate respectively.

$$\frac{1}{\text{wear rate}} = +35.18630 + 15.72190 \times A + 1.42521 \times B + 1.79422 \times C + 1.38812 \times AB + 5.93159 \times A^2 - 0.82389 \times B^2 \quad (4)$$

3.4.1 Influence of Pre-processing Parameters on Wear Rate

From the 3-D surface and 2-D contour plots in Figure 7 (a) and (b), the influence of SRF & SOT on wear rate is illustrated. The lowest wear rate was observed at 10 % silicon carbide weight and 1300 °C surface oxidation temperature. Wear rate decreased with increasing SiC reinforcement fraction (Jafari *et al.*, 2018) at all surface oxidation temperatures. At constant silicon carbide weight, the wear rate at high surface oxidation temperature is lower than those at low oxidation temperature. This implies that silicon carbide weight imposes more influence on the wear resistance property of the composites than surface oxidation temperature as described using equation 4.

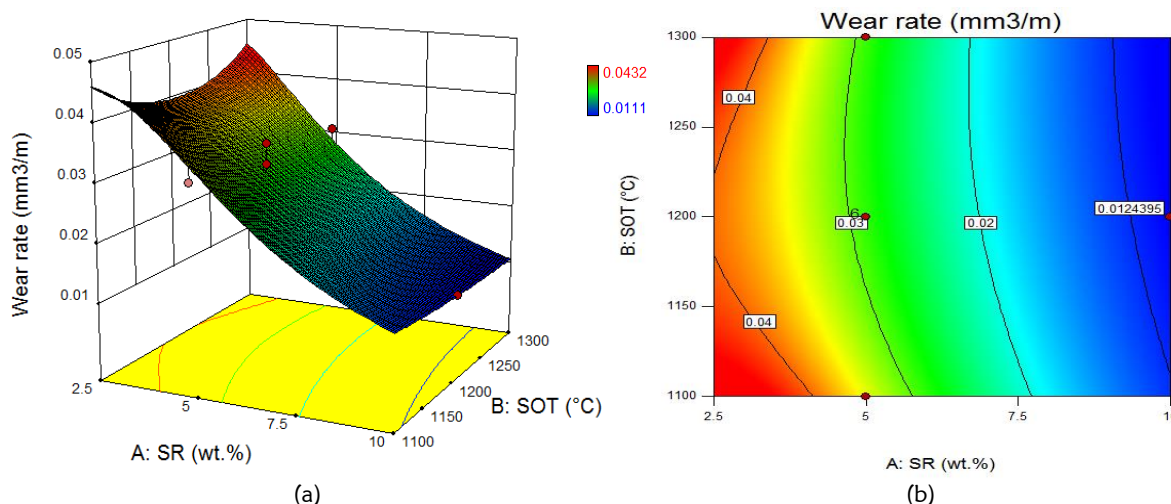


Figure 7: (a) 3-D surface plot, and (b) 2-D contour plot showing the variation of wear rate with silicon carbide reinforcement fraction and surface oxidation temperature

3.5 Model for Coefficient of Friction (μ)

Fit summary statistics of the model for coefficient of friction is shown in Table 7. From the table, the suggested quadratic polynomial for coefficient of friction has F-value of 3.54 at significant p-value of ≤ 0.0612 . Analysis of variance (ANOVA) for coefficient of friction carried out at 5 % significance level is presented in Table 8. From the table, it is observed that the model is significant with a p-value of 0.0001 which is less than 0.05 and F-value of 42.42. A, C, AB, A² and A²B are statistically significant model terms since their p-values are less than 0.05, while, B is an insignificant model term. Other model terms AC, BC, B² and C² were removed for model reduction. Furthermore, the p-value of the lack of fit which corresponds to 0.1561 is greater than 0.05 indicating that the lack of fit is non-significant which is desirable for model adequacy. Also, the difference between the predicted R² (0.8179) and adjusted R² (0.9325) of the model is less than 0.2, which establishes a reasonable agreement as required for model adequacy.

Table 7: Fit summary statistics for coefficient of friction

Source	Sum of Squares	df	Mean Square	F Value	p-value (Prob >F)	
Mean	8.58	1	8.58			
Linear	0.25	3	0.082	16.13	< 0.0001	
2FI	0.028	3	9.362E-003	2.34	0.1244	
<u>Quadratic</u>	<u>0.026</u>	<u>3</u>	<u>8.646E-003</u>	<u>3.54</u>	<u>0.0612</u>	<u>Suggested</u>
Cubic	0.019	4	4.713E-003	7.54	0.0240	Aliased
Residual	3.127E-003	5	6.254E-004			
Total	8.90	19	0.47			

Equation 5 is the model equation developed for the prediction of coefficient of friction (μ) for any given level of each of the process parameters in the experiment. The relative impact of processing parameters on coefficient of friction is identified by comparing their coefficients using equation 6. From the equation, it is concluded that the process parameter with the most influence on COF is silicon carbide reinforcement fraction (SRF). SRF had 35.48 % influence on COF, while SOT and PT had 0.047 % and 2.66 % influence on COF respectively.

$$\mu = +3.85180 - 1.61768 \times SRF - 2.43000E - 003 \times SOT - 4.53750E - 004 \times PT + 1.37100E - 003 \times SRF \times SOT + 0.20929 \times SRF^2 - 1.80400E - 004 \times SRF^2 \times SOT \tag{5}$$

$$\mu = +0.71 - 0.11 \times A - 4.25E - 003 \times B - 0.023 \times C - 0.054 \times AB - 0.045 \times A^2 - 0.056 \times A^2B \tag{6}$$

Table 8: Analysis of variance for coefficient of friction

Source	Sum of Squares	Df	Mean Square	F Value	p-value (Prob > F)	
Model	0.31	6	0.051	42.42	< 0.0001	Significant
A-SiC reinforcement fraction	0.11	1	0.11	92.22	< 0.0001	
B-Surface oxidation temp	1.445E-004	1	1.445E-004	0.12	0.7351	
C-Preheat temp	8.236E-003	1	8.236E-003	6.83	0.0226	
AB	0.023	1	0.023	19.44	0.0009	
A ²	0.025	1	0.025	21.07	0.0006	
A ² B	0.013	1	0.013	10.55	0.0070	
Residual	0.014	12	1.205E-003			
Lack of Fit	0.011	7	1.619E-003	2.59	0.1561	not significant
Pure Error	3.127E-003	5	6.254E-004			
Cor Total	0.32	18				

3.5.1 Influence of Pre-processing Parameters on COF

From the 3-D surface and 2-D contour plots shown in Figure 8 (a) and (b) respectively, influence of SiC reinforcement fraction (SRF) & surface oxidation temperature (SOT) on coefficient of friction (μ) can be observed. The lowest coefficient of friction was observed at 10 % silicon carbide weight and 1300 °C surface oxidation temperature. At silicon carbide weight above 6.7 % and surface oxidation temperatures above 1150 °C, the coefficient of friction was observed to be decreasing.

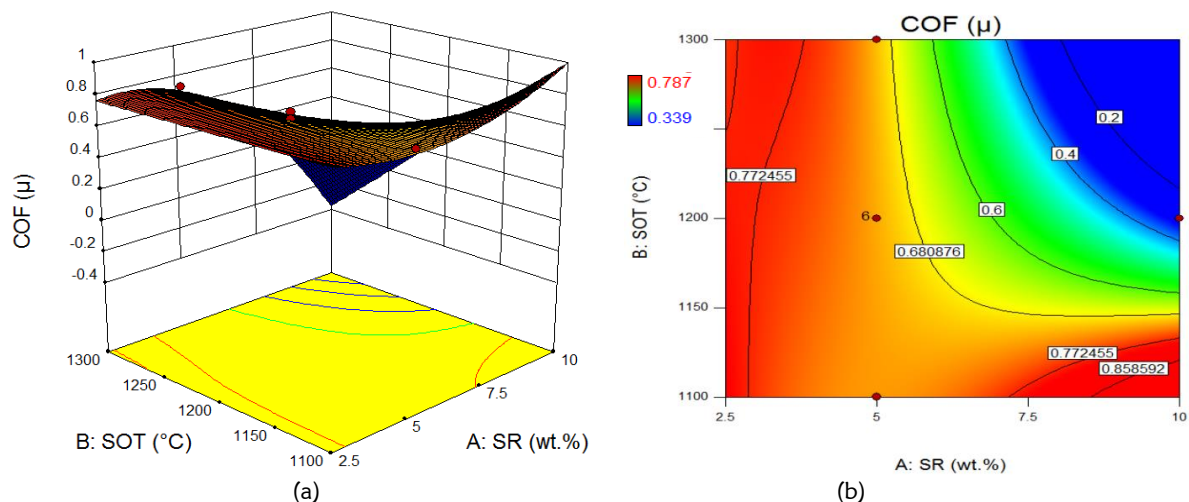


Figure 8: (a) 3-D surface plot, and (b) 2-D contour plot showing the variation of coefficient of friction with silicon carbide weight and surface oxidation temperature

3.6 Surface Characteristics of Worn Samples

The surface characteristics of worn AA6061/oxidized-SiC_p composite samples with the minimum and maximum wear rates were investigated with the unreinforced AA6061 alloy using optical microscopy. For the unreinforced AA6061 alloy shown in Figure 9 (a), the wear scars reveal extensive plastic deformation producing deeper micro-cutting on the worn surface indicating adhesive wear. This is attributed to the lack of adequate strength by the alloy to overcome the applied load exerted by the static partner (stainless steel ball). Figure 9 (b) shows the AA6061/2.5wt.% oxidized-SiC_p composite (experiment run 17) which had the highest wear loss of all the composite samples tested. From the micrograph, it can be observed that the sample has similar wear surface characteristics to the unreinforced AA6061 alloy but exhibited mild adhesive marks and craters on its worn surface. From the micrograph of AA6061/10wt.% oxidized-SiC_p composite sample (experiment run 13) which had the least wear rate in Figure 9 (c), it can be observed that the sample had continuous scratches on its worn surface suggesting mild abrasive wear with few shallow grooves and craters when compared to other samples. This may be attributed to larger quantity of SiC_p reinforcement particles present in the composite material which may have improved the load bearing strength of the composite, thereby reducing its plastic deformation. (Jafari *et al.*, 2018; Vantrinh *et al.*, 2018).

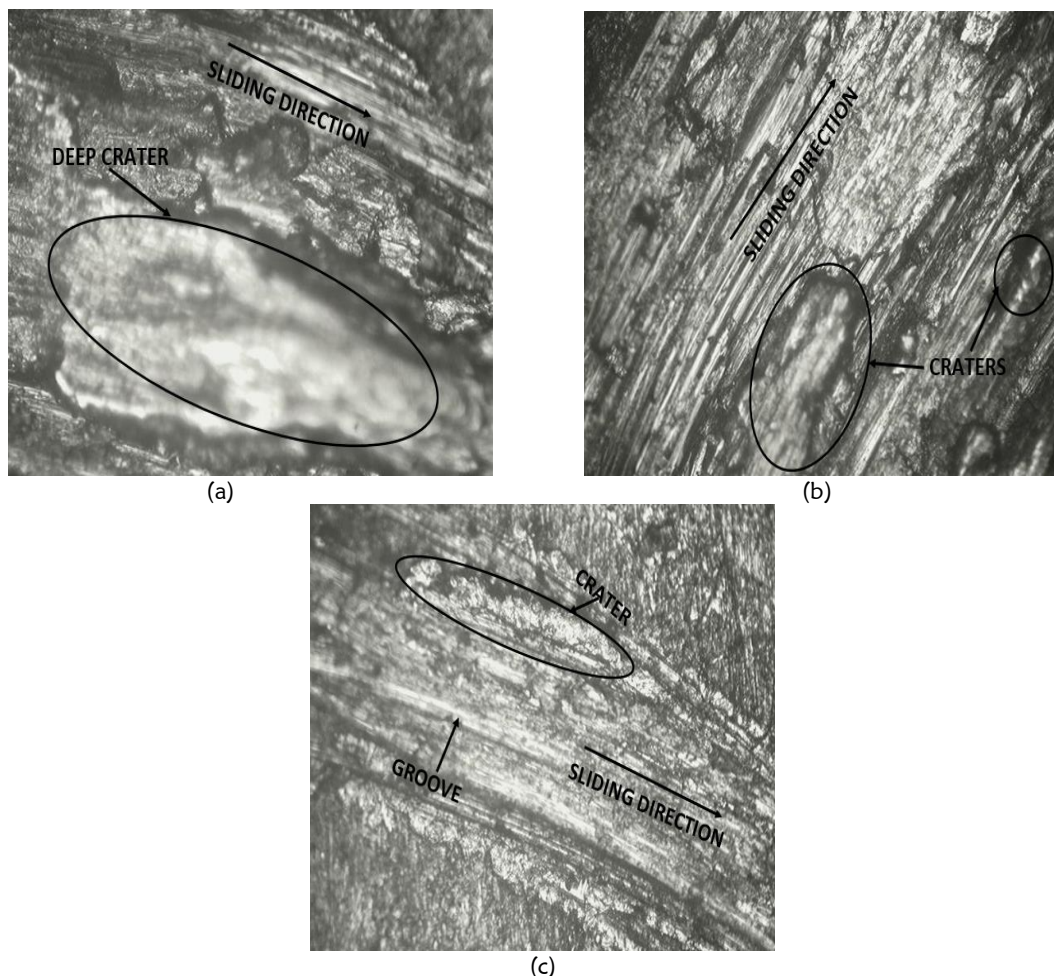


Figure 9: Micrograph wear worn surfaces of (a) AA6061 alloy, (b) AA6061/2.5 wt.% oxidized-SiC_p composite and (c) AA6061/10 wt.% oxidized-SiC_p

4 MULTI-OBJECTIVE OPTIMIZATION (MOO) ANALYSIS

The two models obtained in equation 3 and 5 can be used to generate points of desirable results in the design region for wear rate and COF respectively, since the required process condition for one response is different from the other. However, this can be overcome through utilization of multi-objective optimization (MOO), a tool in RSM where both responses (wear rate and COF) are simultaneously optimized. For this research, the goal was to minimize both wear rate and COF at a specific combination of input factors being considered. Based on the solution analysis in Table 9, optimum values of input process parameters is achieved with experiment number 1 and the ramp graph showing the details of the input factors and the corresponding responses is shown in Figure 10. From Table 9 and Figure 10, the optimum influence of pre-processing parameters on the tribological behaviour of Al-SiC_p composites obtained from the MOO are 9.907% SiC reinforcement fraction, 1233.993 °C surface oxidation temperature, and 376.183 °C preheat temperature. The resulting responses at this optimized condition are 0.110 mm³/m for wear rate and 0.110 for COF with a confidence and desirability level of 1.

Table 9: Optimal solution generated for the response

Solution Number	SiC Reinforcement Fraction	Surface Oxidation Temp.	Preheat Temp.	Wear Rate	Coefficient of Friction	Desirability	
1	<u>9.907</u>	<u>1233.993</u>	<u>376.183</u>	<u>0.011</u>	<u>0.110</u>	<u>1.000</u>	<u>Selected</u>
2	9.997	1227.829	345.497	0.011	0.149	1.000	
3	10.000	1216.667	436.667	0.011	0.183	1.000	
4	9.996	1215.850	476.076	0.011	0.171	1.000	
5	9.867	1210.665	496.646	0.011	0.215	1.000	

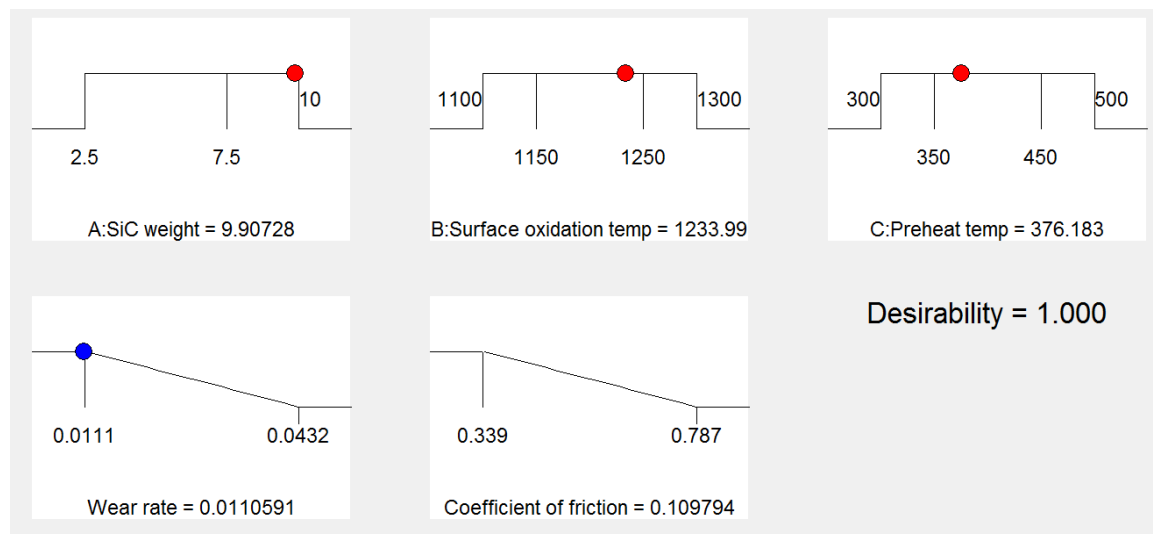


Figure 10: Ramp graph at optimal solution

5 CONCLUSIONS

Based on the results obtained in this research, the following conclusions were drawn:

1. Optimum condition for reinforcement pre-processing in Al-SiC_p composite development was successfully achieved using the CCD.
2. Based on central composite design of RSM, empirical models capable of evaluating the properties wear rate and COF under various reinforcement pre-processing parameter conditions were developed.
3. Analysis of variance (ANOVA) was used to test the adequacy of the developed models at 95% confidence level and the models were found to be significant and adequate. From the 3-D & 2-D surface plots for wear rate, the influence of SRF & SOT on wear rate was analyzed.
4. The wear rate was observed to decrease with increasing silicon carbide weight at all surface oxidation temperatures. At 44.49 %, SRF had the most influence on wear rate, while SOT and PT had 0.65 % and 1.03 % influence on wear rate respectively.
5. For the surface plots showing the influence of SRF & SOT on coefficient of friction, the lowest COF was observed at 10% silicon carbide weight and 1300 °C surface oxidation temperature. At silicon carbide weight above 6.7% and surface oxidation temperatures above 1150 °C, the coefficient of friction was observed to be decreasing. At 35.48 %, SRF had highest influence on COF, while SOT and PT had 0.047 % and 2.66 % influence on COF respectively.
6. From the optimization analysis, the set of conditions that simultaneously optimizes both wear rate and COF was found as 9.907% SiC reinforcement fraction (SRF), 1233.993 °C surface oxidation temperature (SOT), and 376.183 °C preheat temperature (PT). The resulting responses at this optimized condition are 0.110 mm³/m for wear rate and 0.110 for COF with a confidence and desirability level of 1.
7. With result, the AA6061/oxidized-SiC_p composite with superior wear resistance can be utilized for wear resistant applications such as automobile piston.

REFERENCES

1. Adebisi, A. A., Maleque, M. A., Ali, M. Y. & Bello, K. A. (2016). Effect of variable particle size reinforcement on mechanical and wear properties of 6061Al-SiC_p composite. *Composite Interfaces*, 23:6, 533-547. DOI:10.1080/09276440.2016.1167414.
2. Adebisi, A. A., Maleque, M. A., & Bello, K. A. (2017). Investigation of parametric influence on the properties of Al6061-SiC_p composite. *IOP Conf. Series: Materials Science and Engineering* 184 (2017) 012019. doi:10.1088/1757-899X/184/1/012019.
3. Adebisi, A. A., Ndaliman, M. B. (2015). Mathematical Modelling of Stir Casting Process Parameters for Al-SiC_p Composite using Central Composite Design. *Proceedings of the 28th AGM and International Conference of the Nigerian Institution for Mechanical Engineers*. Hosted by The Nigerian Institution for Mechanical Engineers, ABUJA City, Nigeria, October 21-23, 2015.
4. Adediran, A. A., Akinwande, A. A., Balogun, O. A., Olorunfemi, B. J. (2021). Optimization studies of stir casting parameters and mechanical properties of TiO₂ reinforced Al 7075 composite using response surface methodology. *Sci Rep.* 2021 Oct 6;11(1):19860. doi: 10.1038/s41598-021-99168-1. PMID: 34615935; PMCID: PMC8494885.

5. Ahmad, A., Lajis, M. A., Yusuf, N. K. and Rahim, S. N. (2020). Statistical Optimization by the Response Surface Methodology of Direct Recycled Aluminum-Alumina Metal Matrix Composite (MMC-AIR) Employing the Metal Forming Process. *Processes* 2020, 8, 805.
6. Alten, A., Erzi, E., Gürsoy, Ö., Ağaoğlu, G. H., Dispınar, D. and Orhan, G. (2019). Production and mechanical characterization of Ni-coated carbon fibers reinforced Al-6063 alloy matrix composites. *Journal of Alloys and Compounds* (2019).
7. Bobić, B., Mitrović, S., Babić, M., I. Bobić, I. (2010). Corrosion of Metal-Matrix Composites with Aluminium Alloy Substrate. *Tribology in industry*, Volume 32, No. 1, 2010.
8. Jafari, F., Sharifi, H., Saeri, M. R. & Tayebi, M. (2018). Effect of Reinforcement Volume Fraction on the Wear Behavior of Al-SiCp Composites Prepared by Spark Plasma Sintering. *Silicon*. <https://doi.org/10.1007/s12633-018-9779-2>.
9. Di Leo, G., Sardanelli, F. (2020). Statistical significance: p value, 0.05 threshold, and applications to radiomics—reasons for a conservative approach. *Eur Radiol Exp* 4, 18 (2020). <https://doi.org/10.1186/s41747-020-0145-y>.
10. Khalid, M. G., Liaqat, A., Akhlaq, A., Rafiq, A., Kashif, M. D., Ijaz, A. C. & Ramzan, A. K. (2013). Synthesis and Characterization of Al/SiC Composite Made by Stir Casting Method. *Pak. J. Engg. & Appl. Sci.* Vol. 12, Jan., 2013 (p. 102-110) 102.
11. Lee, T., Lee, J., Lee, D., Jo, I., Lee, S. K. & Ryu, H. J. (2020). Effects of particle size and surface modification of SiC on the wear behavior of high volume fraction Al/SiCp composites. *Journal of Alloys and Compounds* 831 (2020) 154647.
12. Montgomery, D. C. (2013). *Design and Analysis of Experiments*; Eighth Edition. John Wiley & Sons, Inc., 111 River Street, Hoboken, New Jersey.
13. Moses, J. J., Dinaharan, I., Sekhar, S. J. (2016). Prediction of influence of process parameters on tensile strength of AA6061/TiC aluminum matrix composites produced using stir casting. *Trans. Nonferrous Met. Soc. China* 26(2016) 1498–1511.
14. Myers, R. H., Montgomery, D. C. and Anderson-Cook, C. M. (2016). *Response Surface Methodology: Process and Product Optimization Using Designed Experiments*; Fourth Edition. John Wiley & Sons, Inc., Hoboken, New Jersey
15. Nagaral, M., Auradi, V., Parashivamurthy, K.I. and Kori, S.A. (2016). A Comparative Study on Wear Behavior of Al6061-6% SiC and Al606 1-6% Graphite Composites. *Journal of Applied Mechanical Engineering* 2016, 5:6.
16. Odiwo, H., Bello, K.A., Abdulwahab, M., Adebisi, A.A. & Maleque, M.A. (2021). Properties of Aluminium/Electroless Ni-Coated SiC Composites - A Review. *FUDMA Journal of Sciences (FJS)*, Vol. 5 No. 1, March, 2021, pp 381 – 394.
17. Ramesh, C.S., Keshavamurthy, R., Channabasappa, B.H. & Pramod, S. (2010). Friction and Wear Behavior of Ni-P coated Si₃N₄ reinforced Al6061 composites. *Tribology International* 43 (2010), 623 – 634.
18. Rana, R. S., Purohit, R., Mishra, P. M., Sahu, P. & Dwivedi, S. (2017). Optimization of Mechanical Properties of AA 5083 Nano SiC Composites using Design of Experiment Technique. 5th International Conference of Materials Processing and Characterization (ICMPC 2016). *Materials Today: Proceedings* 4 (2017) 3882–3890.
19. Umanath, K., Palanikumar, K., & Selvamani, S.T. (2013). Analysis of dry sliding wear behaviour of Al6061/SiC/Al₂O₃ hybrid metal matrix composites. *Composites: Part B* 53 (2013) 159–168.
20. Vantrinh, P., Lee, J., Minh, P. N., Phuong, D. D. & Hong, S. H. (2018). Effect of oxidation of SiC particles on mechanical properties and wear behavior of SiCp/Al6061 composites. *Journal of Alloys and Compounds* 769 (2018), 282-292.
21. Verma, V. and Khvan, A. (2019). Advances in Composite Materials Development. Chapter; A Short Review on Al MMC with Reinforcement Addition Effect on Their Mechanical and Wear Behaviour. InTechOpen.: DOI: <http://dx.doi.org/10.5772/intechopen.83584>